XXI ICTAM, 15–21 August 2004, Warsaw, Poland

GÖRTLER VORTEX SECONDARY STABILITY: VARICOSE MODE

Leandro F. Souza*, Márcio T. Mendonça**, Marcello A. F. Medeiros*, Markus J. Kloker***
* *EESC-USP, Universidade de São Paulo, São Carlos, Brazil*
** *IAE-CTA, Centro Técnico Aeroespacial, São José dos Campos, Brazil*
*** *IAG, Universität Stuttgart, Stuttgart, Germany*

Summary The varicose mode of Görtler vortex secondary instability was investigated using direct numerical simulation. Root mean square of the streamwise, normal and spanwise secondary instability fluctuation velocity components are presented and compared to previous investigations. The horseshoe structure that evolves due to this secondary instability is also presented showing good qualitative agreement with the structures observed experimentally.

INTRODUCTION

The mushroom type structures that develop due to Görtler vortices result in strongly inflectional streamwise velocity profiles both in the normal and spanwise directions. As a result, secondary instability sets in either as a sinuous or a varicose mode [1]. Hall and Horseman [2] studied both types of secondary instability using an inviscid model and presented the corresponding eigenfunctions. Their results were confirmed by the viscous parallel model of Yu and Liu [3]. A more comprehensive study was presented by Li and Malik [4]. They identified more than one fundamental mode and subharmonic modes that have growth rates comparable to those of the fundamental modes. Their results showed that the sinuous mode is stronger initially, but further downstream the varicose mode has stronger growth rates than the sinuous mode. The present study investigates, through direct numerical simulation, the development of the varicose mode observed in the experiment of Swearingen and Blackwelder [1]. Streamwise, normal and spanwise velocity fluctuations were analyzed and compared to results from previous investigations. The horse-shoe type structure was similar to the structure observed experimentally [1].

FORMULATION AND NUMERICAL METHOD

In the present study the complete Navier-Stokes equations for a constant density and viscosity fluid were rewritten in a vorticity-velocity formulation [5] for the disturbances. The Blasius boundary layer was used as the base flow. The governing equations in non-dimensional form leads to the appearance of the Görtler number, $Go = (k_c\sqrt{Re})^{1/2}$, where k_c is the curvature of the wall. The reference length and reference velocity were L and U_∞, the free-stream velocity. The Reynolds number was given by $Re = U_\infty L/\nu$.

At the wall, no-slip and no penetration boundary conditions were imposed. Disturbances were introduced into the flow field using a suction and blowing function at the wall in a disturbance strip [5]. At the inflow, the velocity and vorticity components were specified based on the Blasius boundary layer. At the upper boundary, the vorticity disturbances were assumed to decay exponentially to zero. A buffer domain technique was implemented in order to avoid wave reflections in the outflow boundary [6].

The equations were solved numerically on an orthogonal uniform grid. The time derivatives were integrated with a classical 4^{th} order Runge-Kutta scheme. The spatial derivatives were calculated using a 6^{th} order compact finite difference scheme. The flow was assumed to be periodic in the spanwise (z) direction and symmetric with respect to $z = 0$. Therefore, the disturbances were expanded in real Fourier cosine and sine series.

RESULTS

In current study the parameters were identical to those used in the experiment of Swearingen e Blackwelder [1]. In their experiment a non stationary disturbance of 130 Hz was observed, and a disturbance with this frequency was introduced in the present numerical simulation. Figures 1 to 3 present the root mean square (rms) of the non stationary disturbance velocity components in the streamwise, normal and spanwise directions at the streamwise position $x = 11.02$ cm. In this figures the mean streamwise velocity profile due to the Görtler vortices is also shown by dashed contour lines, varying from 0.1 to 0.9.

In Figure 1 the largest value of the u_{rms} of about 3.6% is located at the central region ($z = 0$). This u_{rms} peak is located above the wall exactly where the mean flow streamwise velocity is $0.7U_\infty$. This is also the location of the inflection point in the streamwise mean velocity component. This result are in qualitative agreement with the results obtained by [2, 3] and [4] for the first varicose mode, with a single dominant peak at the head of the mushroom. The weaker peaks close to the wall were not capture by Li's [4] inviscid analysis. In the same paper [4] nonlinear, viscous results indicate that the peaks close to the wall grow as the instability develops downstream.

The normal and spanwise disturbance velocity components have more complex structures with stronger v_{rms} peaks located above and inside the mushroom. The w_{rms} has strong peaks on either sides of the mushroom. Figure 2 presents the isolines of v_{rms}. Again, the results are in qualitative agreement with [2] and [3], with a velocity peak at the center.

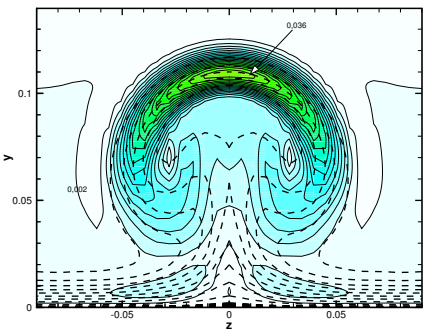

Figure 1. Contour: u_{rms}. Dashed: $\bar{u}$.

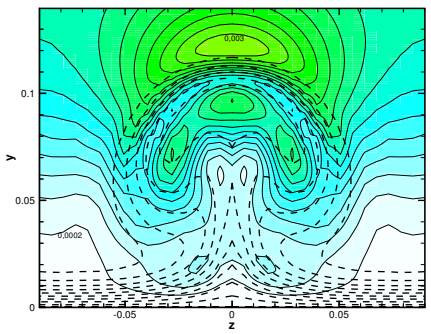

Figure 2. Contour: v_{rms}. Dashed: $\bar{u}$.

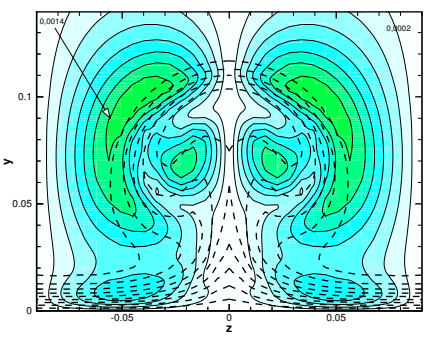

Figure 3. Contour: w_{rms}. Dashed: $\bar{u}$.

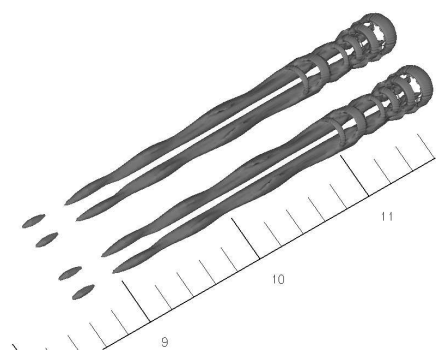

Figure 4. The horseshoe structure.

But in the present study the largest amplitudes of the v_{rms} occurred above the mushroom structure. This difference may be because [2] and [3] considered a parallel mean flow for the secondary stability analysis, discarding the normal and spanwise velocity components of the mushroom.

The results for w_{rm} shown in Figure 3 are also in qualitative agreement with the analysis of [3]. In the present results the two peaks on either side of the mushroom head are farther apart from each other when compared to the results from [3]. These peaks are located at the outer layer of the mushroom, while in [3] they are located inside the mushroom structure. Again, this discrepancy with [3] may be attributed to the parallel assumption used in that work.

In Figure 4 Q isosurfaces are shown for a given time t. The Q isosurfaces are obtained by the method described in [7] and represent the vortical structure of the flow. The streamwise extent covers a region from earlier nonlinear Görtler vortex up to the secondary instability region. These structures were also observed in the experiment of Swearingen and Blackwelder [1].

CONCLUSIONS

In this work the secondary stability of Görtler vortices to non stationary disturbances were analyzed. The results were in good agreement with results from previous investigations. Direct numerical simulation model was able to take into account nonlinear, nonparallel and viscous effects. The mushroom structures observed in the experiment of Swearingen and Blackwelder [1] were recovered in the numerical simulation. Future work will investigate also the sinuous mode and the effect of the spanwise wavelength. The financial support from FAPESP (State of Sao Paulo Research Support Foundation) – Grant numbers 00/04943-7 and 03/05027-2 – is greatly acknowledged.

References

[1] Swearingen J. D., Blackwelder R. F.: The Growth and Breakdown of Streamwise Vortices in the Presence of a Wall. *J. Fluid Mech.*, **182**:255, 1987.

[2] Hall P., Horseman N. J.: The Linear Inviscid Secondary Instability of Longitudinal Vortex Structures in Boundary Layers. *J. Fluid Mech* **232**:357–375, 1991.

[3] Yu X., Liu J. T. C.: On the Mechanism of Sinuous and Varicose Modes in Three-Dimensional Viscous Secondary Instability of Nonlinear Görtler rolls *Physics of Fluids*, **6**:736–750, 1994.

[4] Li F., Malik M. R.: Fundamental and Subharmonic Secondary Instability of Görtler Vortices. *J. Fluid Mech* **297**:77–100, 1995.

[5] Meitz H. L., Fasel H. F.: A compact-difference scheme for the Navier-Stokes equations in vorticity-velocity formulation. *J. Comp. Phys.*, **157**:371–403, 2000.

[6] Kloker M., Konzelmann U., Fasel H. F.: Outflow Boundary Conditions for Spatial Navier-Stokes Simulations of Transition Boundary Layers. *AIAA Journal*, **31**:620–628, 1993.

[7] Dubief Y., Delvayre F.: On coherent-Vortex Identification in Turbulence. *J. of Turbulence*, **11**:1–22, 2000.